A NEW CONCEPT OF REDUCED-SCALE DYNAMOMETER

Gabriel Aquino Schell Kruze, gabrielkruze@hotmail.com
Patric Daniel Neis, neyferr@gmail.com
Ney Francisco Ferreira, engmecpatric@yahoo.com.br
Universidade Federal do Rio Grande do Sul (UFRGS), Porto Alegre, Brazil.

Luciano Tedesco Matozo, lucianom@fras-le.com.br
Fras-le S/A, Caxias do Sul, Brazil.

Abstract. *This paper is about the development and design of a new concept of reduced-scale dynamometer, the FSD (Fras-le Scale Dynamometer). This dynamometer can, with a single brake system and with a single test, reproduce the behavior of several full-scale brake systems. The objective of this paper was to initially reproduce the performance of four full-scale systems with the FSD, but the idea is to reproduce the performance of nineteen full-scale brake systems in the future. The thermal behavior of the four full-scale systems was compared to the thermal behavior of different FSD disc thicknesses to determine the FSD disc thickness that approximately reproduce the thermal behavior of the four full-scale systems. In this paper, the FSD friction curve was adjusted for every one of the four full-scale systems by a correction factor (moved vertically up or down) to compare the friction coefficient behavior between them.*

Keywords*: Reduced-scale dynamometer, brake system.*

1. INTRODUCTION

The development of new fiction materials to be used in automotive brakes is a constant challenge, because of the increase in engine power and because of higher market requirements. The equipment most utilized during the development stage of pads and linings is the inertial dynamometer, which is a machine capable of generating performance results very similar to the vehicles'. However, dynamometers are costly and the test time for every system can last several days. So using an inertial dynamometer in the design of new friction materials can be expensive and very time consuming.

To minimize costs, reduced-scale dynamometers were made. They work with a scale factor to reproduce results of full-scale brake systems, but these machines reproduce the results of a single full-scale system, with a correspondent scale factor for this system. So UFRGS (Universidade Federal do Rio Grande do Sul), together with Fras-le S/A from Caxias do Sul, have developed a reduced-scale dynamometer with a fixed scale factor and the results of this machine can be used to reproduce the results of several full-scale systems with a single test. This equipment was called *Fras-le Scale Dynamometer* (FSD) and its development has financial support of FINEP (Financiadora de Estudos e Projetos).

The tests done during the development stage of new friction materials could last several days. This occurs because a single friction material should be tested for every brake system. Current dynamometers have been designed to reproduce the results of a single brake system with a test (Fig. 1). The FSD is a reduced-scale dynamometer that with a single brake system and a single test can reproduce the results of several full-scale brake systems (Fig. 2).

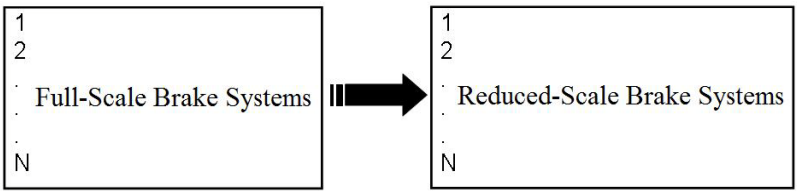

Figure 1. Diagram of the old concept of reduced-scale dynamometers.

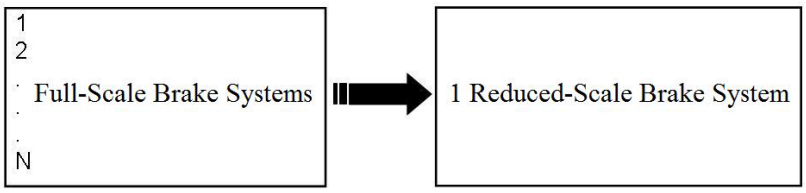

Figure 2. Diagram of the new concept of reduced-scale dynamometer.

The variables that act on brake system performance, friction and wear are: sliding velocity, contact pressure and temperature (Infantini, 2008). The FSD was designed so these variables were similar to nineteen full-scale brake systems. This dynamometer was designed to satisfy more rapidly the development needs of new friction materials, reducing test time and development time of new friction materials. This equipment can be seen in Fig. 3.

Figure 3. *Fras-le Scale Dynamometer*.

So the objective of this paper was to initially reproduce the performance of four full-scale systems with the FSD. However, the idea is to reproduce the performance of nineteen full-scale brake systems in the.

2. EXPERIMENTAL

2.1. Systems Selection

Because of the difficulty in determining the pressure distribution on drum brakes (Day et al., 1984; Day, 1988; Day, 1991; Day et al., 1991; Millner and Parsons, 1973; Susin et al., 2007; Yoshioka, 2007), we decided to consider only disc brakes in this paper. To design the FSD brake system, nineteen disc brake systems were used: twelve lights (A-L), four SUVs (M-P) and three pneumatics (Q-S). Tab. 1 presents a list of four disc brake systems, all of them light vehicles (B to E), considered to be reproduced by the FSD, where the B system is a solid disc system, and the others systems (C, D and E) are vented discs.

Table 1. Used disc brake systems.

System	Disc			Area [cm^2]		Radius					Cylinder (piston)				Inertia [kgm^2]
				Pad		Pad [mm]				Tire [m]	Quantity	Ø [mm]	Reffective [mm]	Area [m^2]	
	Ø [mm]	Thickness [mm]	S or V	Unit	Double	Min	Max	Average	Height						
B	239	12	S	37	74	79	114	96.5	35	0.280	1	48	96	0.0018	50
C	240	20	V	43	86	75	120	97.5	45	0.281	1	48	96.5	0.0018	40
D	255	25	V	46	92	80	127	103.5	47	0.296	1	57	103.5	0.0026	45
E	239	20	V	38.15	76.3	70	116	93	46	0.280	1	54	96	0.0023	50

S – solid disc V – vented disc

2.2. FSD Design

The FSD pad area has 16 cm^2, so it can be cut from the smaller commercial pad and its geometry was defined in a way to minimize errors of sliding velocity of FSD in relation to the full-scale systems (about 13%).

The scale factor represents the relation between pad area of full-scale systems and reduced-scale dynamometer and it was calculated by the Eq. (1) (Wilson et al., 1968; Wilson and Bowsher, 1971; Sanders et al., 2001):

$$S = \frac{A}{a} \tag{1}$$

where:

S = scale factor [ ];
A = arithmetic mean of twelve light systems and four SUVs pads areas [m^2];
a = pad area of FSD [m^2].

The effective radius, or the distance between the axis center and pad center, can be calculated from Eq. (2) (Wilson et al., 1968; Wilson and Bowsher, 1971; Sanders et al., 2001):

$$R_{FSD} = \overline{R}_e \cdot S^{\frac{1}{2}} \tag{2}$$

where:
$\overline{R}_e$ = arithmetic mean of twelve selected light systems [m];
R_{FSD} = effective radius of the FSD [m].

The reduced-scale disc of the FSD was manufactured in cast iron and its diameter was calculated from Eq. (3):

$$D = 2 \cdot R_{effect} + h_{pad} + 2 \tag{3}$$

where:
D = FSD disc diameter [mm];
R_{effect} = effective radii of the FSD pad [mm];
h_{pad} = FSD pad height [mm].

2.3. FSD Thermal Behavior Adjustment

The test procedure used to choose the FSD disc thickness can be seen in Tab. 2, whose operation parameters were defined based on the survey of the sliding velocities and contact pressures of the systems for vehicle velocities and hydraulic pressures given by the AK-Master specification. The inertia used in this test was of 8 kgm^2 to guarantee that the energy density by unit area of the FSD pad was the same for all full-scale systems. The material used in all tests was the same, and it was an organic NAO material.

Another criterion utilized to select the FSD disc thickness, besides the similarity of its thermal behavior in relation to the full-scale systems, was the fade braking initial and final temperatures. For the initial temperature in a braking of the fade stage to be equal to the temperature of the brake procedure (Tab. 2), the final temperature in a previous fade stage braking should be greater than the initial temperature of the next braking.

Table 2. Test procedure.

Stage	Number of Brakings	SLIDING VELOCITY [m/s]		CONTACT PRESSURE [bar]	TEMPERATURE [ºC]
		Initial	Final	Pcontact	Tinitial
Bedding	50	7.4	2.8	13.2	100
Speed 1	7	3.7	0.5	8.8 - 13.2 - 17.7 - 22.1 - 26.5 - 30.9 - 35.3	100
Speed 2	7	7.4	3.7	8.8 - 13.2 - 17.7 - 22.1 - 26.5 - 30.9 - 35.3	100
Speed 3	7	11.1	7.4	8.8 - 13.2 - 17.7 - 22.1 - 26.5 - 30.9 - 35.3	100
Speed 4	7	14.8	12.0	8.8 - 13.2 - 17.7 - 22.1 - 26.5 - 30.9 - 35.3	100
Speed 5	7	16.6	13.8	8.8 - 13.2 - 17.7 - 22.1 - 26.5 - 30.9 - 35.3	100
Fade	15	9.2	0.5	0.4 g	100 -215 - 283 - 330 - 367 - 398 - 423 - 446 - 465 - 483 - 498 - 513 - 526 - 539 - 550
Characteristic Value	18	7.4	2.8	13.2	100
TOTAL	118	brakings			

To measure the disc temperature of the systems and of the FSD, thermocouples were used. The thermocouples were positioned in the discs following the AK-Master specification. Fig. 4 shows the position of the thermocouple in the solid disc. Considering that the disc has 12 mm of thickness and the hole of the thermocouple has 3 mm of diameter, the

thermocouple was positioned at 4 mm from the disc friction surface. In Fig. 5, it is possible to observe the position of the two thermocouples placed in the vented discs. The thermocouples were positioned at 1 mm from the friction surface. In the case of the FSD discs, the thermocouples were positioned. Like the vented discs (Fig. 5), in spite of they being solid discs.

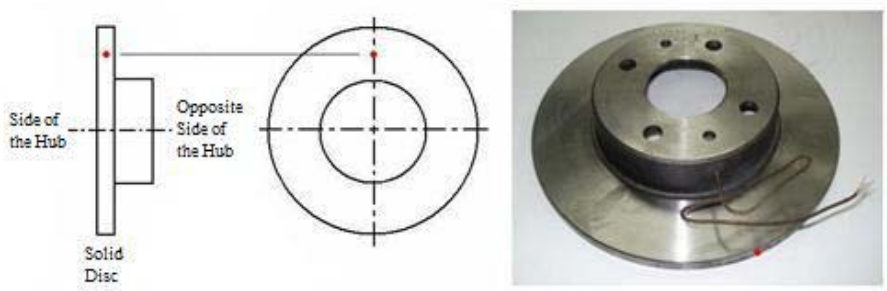

Figure 4. Position of the thermocouple in the system with solid disc.

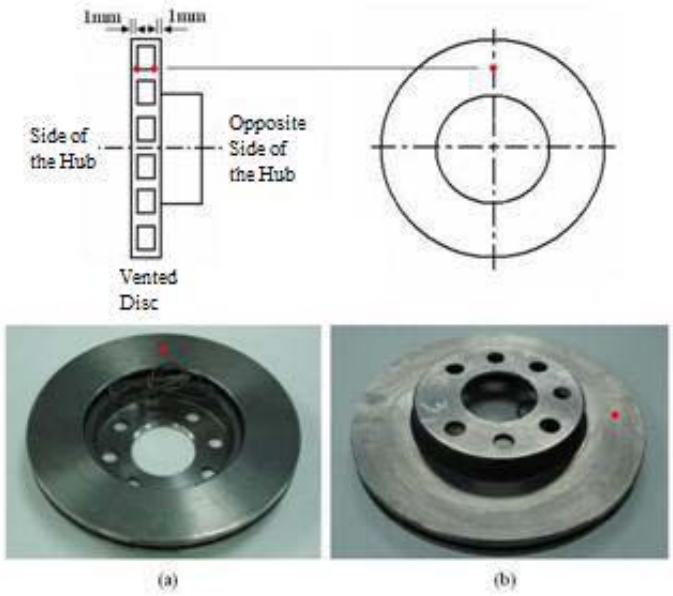

Figure 5. Position of the thermocouples in the systems with vented disc (picture of system C), (a) Side of the hub, (b) Opposite side of the hub.

2.4. FSD Friction Coefficient Behavior Adjustment

To compare the results of the friction coefficient between the full-scale systems (B, C, D and E) and the FSD with the selected 10 mm disc, they were all tested with new pads in the same material, a NAO organic material, and the results of the FSD were moved vertically up or down in a way that the mean friction coefficient of the FSD and of every full-scale system were the same. So the friction curve of the FSD was adjusted to each full-scale system, to compare the friction coefficient in the same level. This was done to compare the results in a qualitative way.

To compare the friction coefficient between the full-scale systems and the adjusted curves of the FSD in a quantitative way, we proposed criteria that were calculated from Eqs. (4), (5), (6) and (7):

$$\%\Delta\mu_{p1-p2} = 100 \cdot \frac{\mu_{p1}-\mu_{p2}}{\mu_{p1}} \tag{4}$$

$$\%\Delta\mu_{v1-v2} = 100 \cdot \frac{\overline{\mu}_{v1}-\overline{\mu}_{v2}}{\overline{\mu}_{v1}} \tag{5}$$

$$\%fade = 100 \cdot \frac{\mu_{bedding} - \mu_{fade}}{\mu_{bedding}} \tag{6}$$

$$\%charact. = 100 \cdot \frac{\mu_{charact.}}{\mu_{bedding}} \quad (7)$$

where:

$\%\Delta\mu_{p1\text{-}p2}$ = friction coefficient sensibility to pressure [%];
$\%\Delta\mu_{v1\text{-}v2}$ = friction coefficient sensibility to velocity [%];
%fade = friction coefficient sensibility to temperature [%];
%caract. = friction coefficient recovery in the last braking of the characteristic value stage in relation to the bedding stage [%];
μ_{p1} = friction coefficient at 30 bar of pressure in the speed 2 stage [ ];
μ_{p2} = friction coefficient at 80 bar of pressure in the speed 2 stage [ ];
$\bar{\mu}_{v1}$ = mean friction coefficient for the pressures of 30 and 80 bar in the speed 2 stage [ ];
$\bar{\mu}_{v2}$ = mean friction coefficient for the pressures of 30 and 80 bar in the speed 4 stage [ ].
$\mu_{bedding}$ = friction coefficient in the last braking of the bedding stage [ ];
$\mu_{caract.}$ = friction coefficient in the last braking of the characteristic value stage [ ];
μ_{fade} = minimum friction coefficient in the fade stage [ ].

3. RESULTS AND DISCUSSION

3.1. FSD Design

With the reduced-scale pad area defined as 16 cm^2 and with the arithmetic mean of the chosen hydraulic systems and SUVs pads areas (98,2 cm^2) the scale factor was calculated from Eq. (1) resulting in a value of approximately 3,1.

With the arithmetic mean of the chosen twelve light systems effective radii (106,3 mm) and the respective scale factor (3,1), the FSD effective radius was calculated from Eq. (2), resulting in a value of approximately 61 mm. The FSD pad thickness was adopted as 11 mm, the same value of Astra or Vectra pad thickness.

With the effective radius (61 mm) and the FSD pad height (35 mm) the diameter of the FSD reduced-scale disc was calculated from Eq. (3), resulting in a value of 159 mm. The additional 2 mm in Eq. (3) is to have a clearance between the FSD pad and the disc edge.

The caliper used in the FSD was the commercial one used in Vectra or Astra rear axe, and the piston diameter of this caliper is 35 mm, so the piston area is 962,11 mm^2. The design of the FSD system brake can be viewed in Fig. 6.

Figure 6. FSD brake system.

3.2. FSD Thermal Behavior Adjustment

The results of the final temperature for the four full-scale brake systems (B, C, D and E), obtained by Infantini (2008), and for the four FSD disc thicknesses is shown in Fig. 7. The temperature of the vented disc systems and of the FSD system is the mean temperature of the two thermocouples at 1 mm from each disc surface. We can verify that the systems do not show considerable differences in temperature, but the solid disc system has slightly higher final temperatures than the vented discs. This is expected because vented discs have internal ventilation fins that help to cool

the disc (Birch, 1999). From Fig. 7, it is possible to observe that the thermal behavior of the 10 mm-thick disc is similar to the thermal behavior of the systems with vented discs (C, D and E).

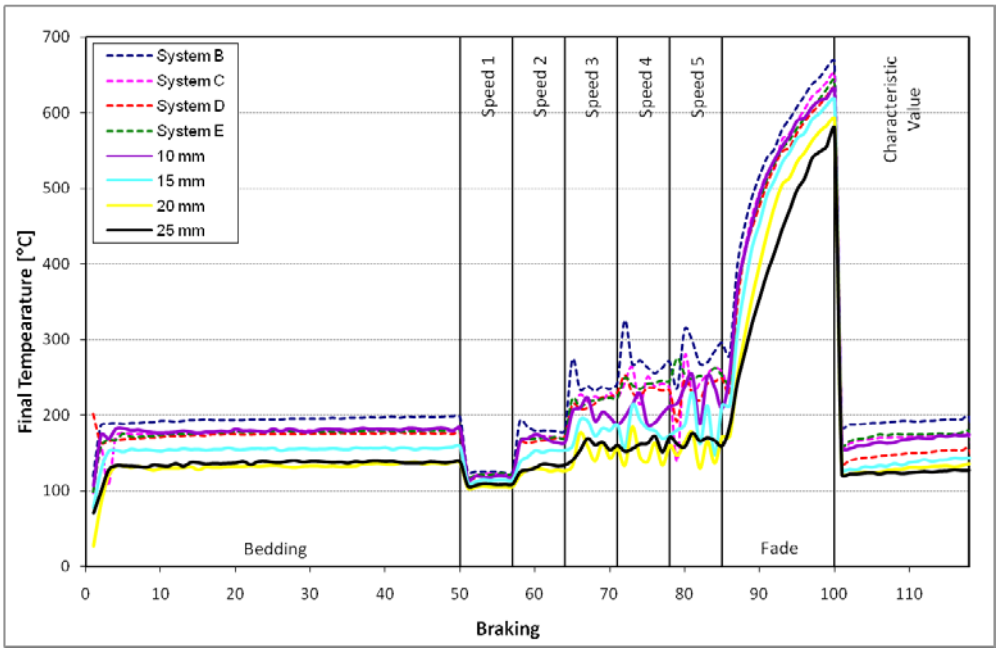

Figure 7. Final temperatures of the full-scale systems and of the different FSD disc thickness.

The thermal behavior of FSD conformed to expectations, because as the FSD disc thickness reduces the final temperature increases. This occurs because as the FSD disc thickness reduces the mass and the thermal inertia of the disc reduces and, consequently, the final temperature measured increases.

In the fade, the 15 mm-thick disc has 213ºC of final temperature at the end of the first braking, but the second braking should initiate at 215ºC, and the disc cools a little before the beginning of the next braking, so it is impossible for the 15 mm-thick disc to achieve the temperature of 215ºC at the beginning of the next fade braking. Therefore, only the 10mm-thick disc could meet this criterion in every fade stage braking, as it can be seen in Tab. 3.

Table 3. Initial and final temperatures of the first five fade brakings for all FSD disc thickness.

FADE STAGES	INITIAL TEMPERATURE [°C]	INITIAL AND FINAL TEMPERATURE [°C]				
	Fade	10 mm	15 mm	20 mm	25 mm	35 mm
1	100	94	95	94	97	95
		256	213	172	185	173
2	215	204	184	163	154	140
		364	307	249	241	225
3	283	266	258	223	200	175
		415	370	305	282	260
4	330	312	317	273	241	205
		456	423	356	321	291
5	367	346	352	321	281	234
		491	455	400	355	321

According to the two criteria mentioned above the selected disc thickness was of 10 mm, because it possesses a thermal behavior similar to the full-scale systems especially with vented discs and can achieve the desired initial temperatures in every fade braking.

3.3. FSD Friction Coefficient Behavior Adjustment

The results of the friction coefficient for the four full-scale systems, obtained by Infantini (2008), and for the FSD can be viewed in Fig. 8. A characteristic behavior of the friction material can be observed at the fade stage for all systems and the FSD, where initially there is a reduction of the friction coefficient with the increase of temperature, and

after this, the friction coefficient starts to increase as temperature rises. This happens because of the degradation of the phenolic resin that occurs at approximately 350ºC (Cristol-Bulthé et al., 2007).

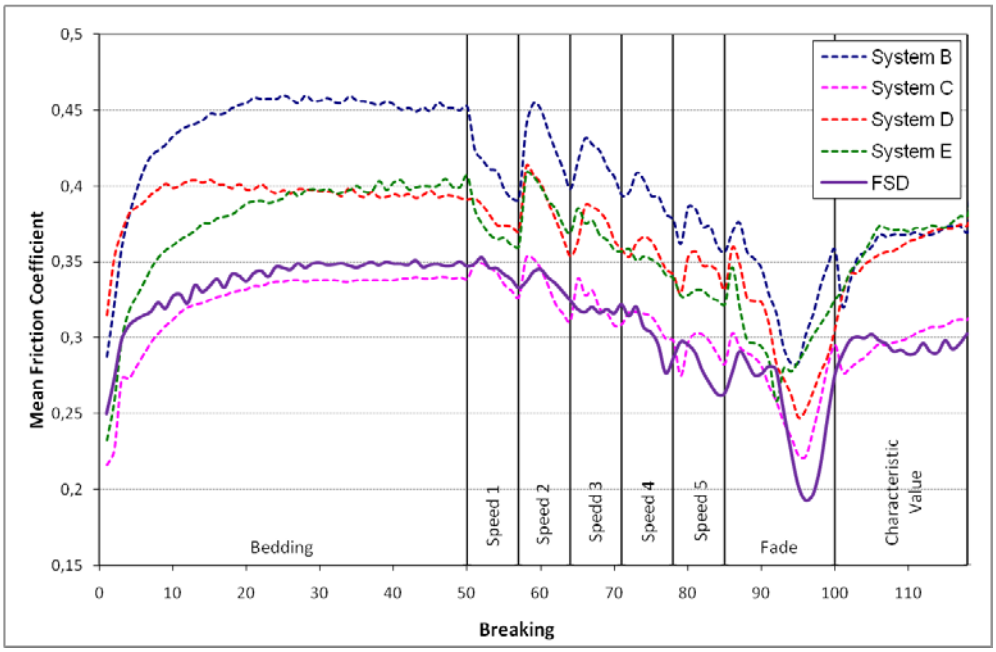

Figure 8. Friction coefficient of the full-scale systems and of the FSD.

The friction coefficient of systems B, C, D and E, together with the FSD friction curves, which were adjusted in relation to each system, can be seen respectively in Figs. 9, 10, 11 and 12. Figs. 9, 10, 11 and 12 show that the FSD has a behavior tendency similar to the other systems but in a different level, so the full-scale systems and the FSD have a similar behavior in a qualitative way.

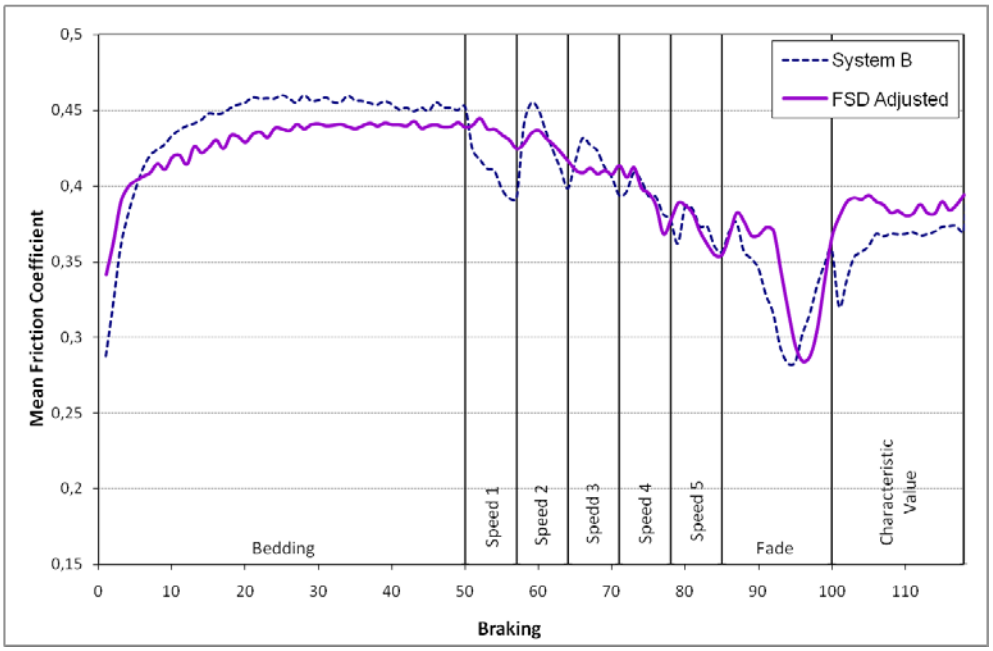

Figure 9. Friction coefficient of system B and of the FSD adjusted to that system.

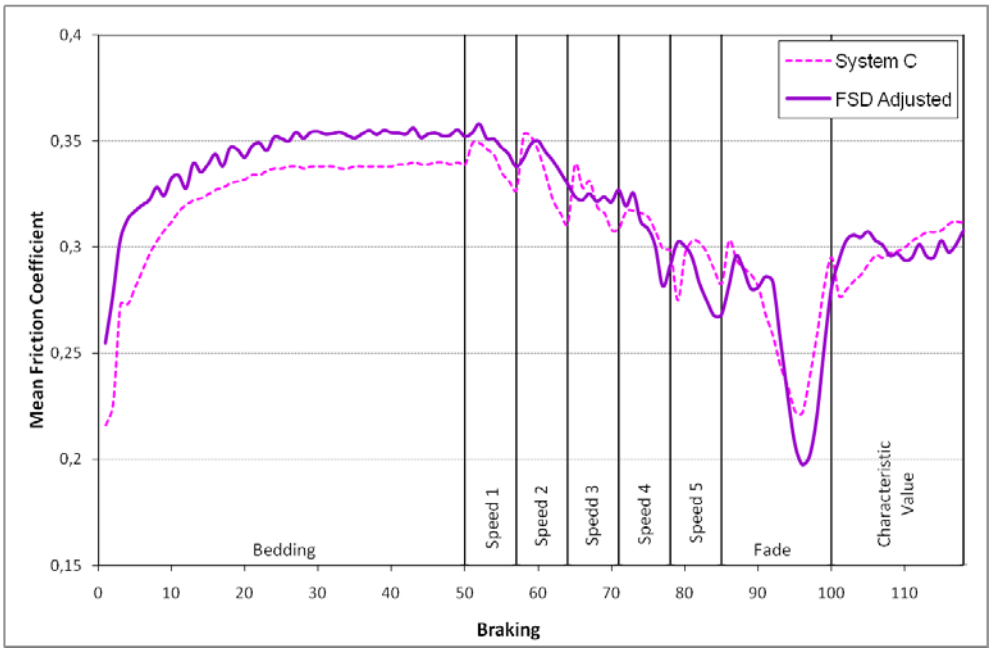

Figure 10. Friction coefficient of system C and of the FSD adjusted to that system.

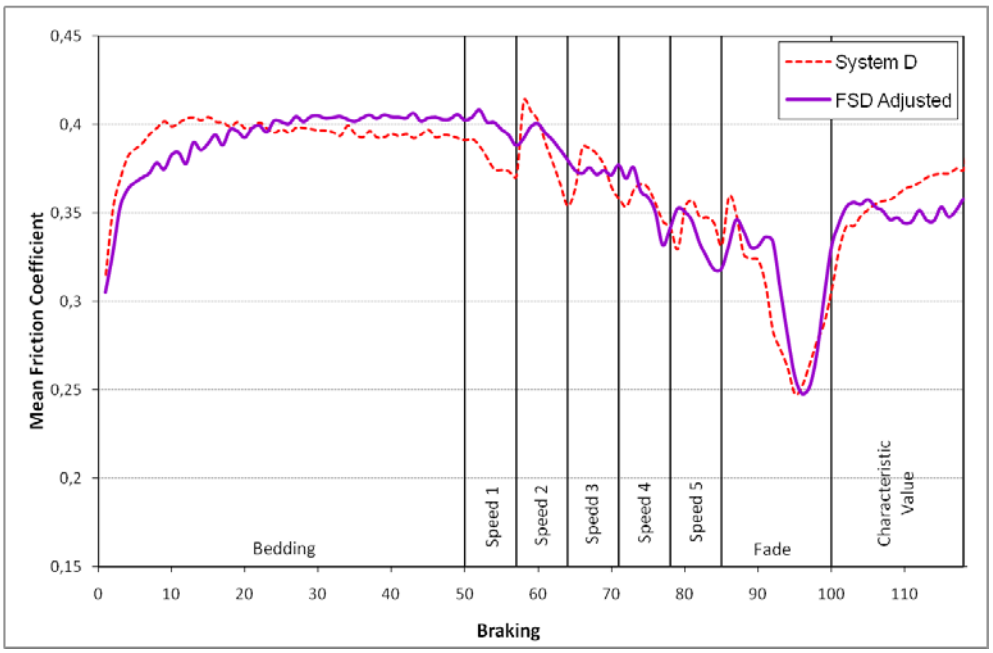

Figure 11. Friction coefficient of system D and of the FSD adjusted to that system.

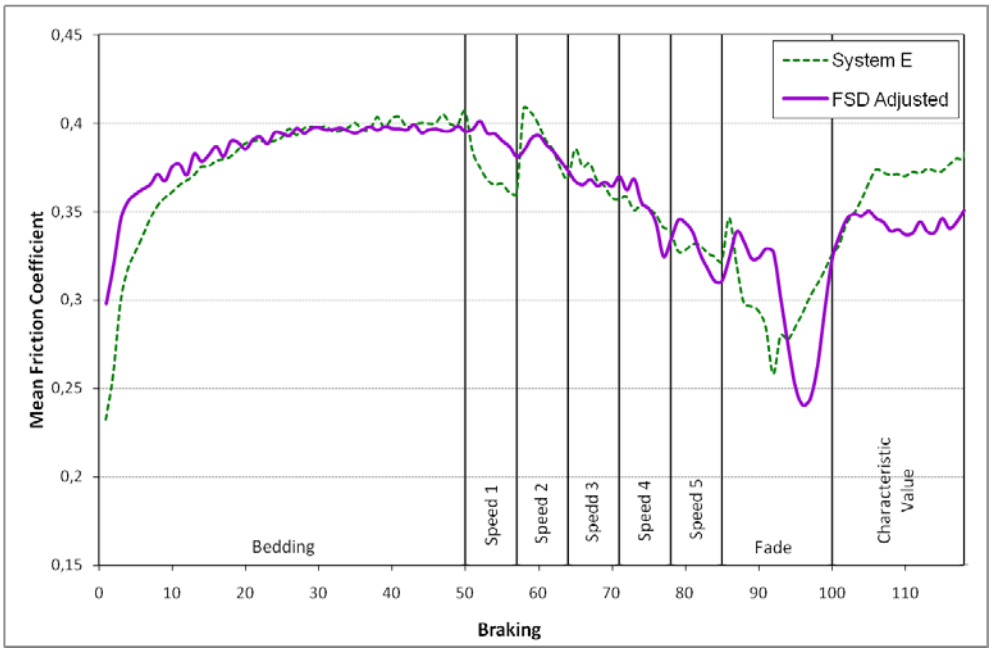

Figure 12. Friction coefficient of system E and of the FSD adjusted to that system.

The results of the criteria calculated from Eqs. (4), (5), (6) and (7) are shown in Tab. 4 for the full-scale systems and for the FSD friction curves adjusted to each system. The results in Tab. 4 show that the friction coefficient sensibility to temperature (*%fade*) and to velocity ($\%\Delta\mu_{v1\text{-}v2}$), and the friction coefficient recovery (*%charact.*) were similar between the full-scale systems and the FSD curves adjusted to each system, but the same did not occur to the friction coefficient sensibility to pressure ($\%\Delta\mu_{p1\text{-}p2}$), where a meaningful difference is observed between the full-scale systems and the FSD adjusted curves for every system.

Table 4. Criteria utilized to compare quantitative the friction coefficient between the full-scale systems and the adjusted curves of the FSD.

	FSD	**System B**	**FSD Adjusted (System B)**	**System C**	**FSD Adjusted (System C)**	**System D**	**FSD Adjusted (System D)**	**System E**	**FSD Adjusted (System E)**
$\%\Delta\mu_{p1\text{-}p2}$	5,36	12,42	4,24	11,65	5,29	13,09	4,62	9,11	4,70
$\%\Delta\mu_{v1\text{-}v2}$	11,42	8,41	8,99	6,52	11,26	7,01	9,81	10,27	10,00
%Fade	44,50	37,33	35,25	34,51	43,87	36,70	38,40	36,49	39,10
%Charact.	87,19	81,78	89,85	92,04	87,37	95,74	88,95	93,62	88,75

4. CONCLUSIONS

The 10 mm-thick disc was selected because it has a thermal behavior similar to the full-scale systems with vented disc and can satisfy the desired initial temperatures in every fade braking.

The FSD adjusted and the full-scale friction curves has a similar behavior but in different levels, manly the decrease of the friction coefficient in the speed stages and in the fade. The decrease of the friction coefficient in the fade occurs because of the degradation of the phenolic resin (Cristol-Bulthé et al., 2007).

The criteria friction coefficient sensibility to temperature (*%fade*) and to velocity ($\%\Delta\mu_{v1\text{-}v2}$) and the friction coefficient recovery (*%charact.*) were similar between the full-scale systems and the adjusted FSD curves, but in the friction coefficient sensibility to pressure ($\%\Delta\mu_{p1\text{-}p2}$) there is a meaningful difference.

To sum up, the reduced-scale dynamometer FSD can reproduce the four selected systems with similar temperatures and friction coefficients, but the friction coefficient should be adjusted as they have similar behavior but in different levels. So the FSD friction curve should be adjusted (moved vertically up or down) by a correction factor for every system to represent each system friction curve. In the future, the idea is to reproduce the performance of nineteen full-scale brake systems with it.

5. REFERENCES

Birch, T. W., 1999. “Automotive Braking Systems”, Third Edition, Delmar.

Cristol-Bulthé, A., Desplanques, Y., Degallaix, G., Berthier, Y., 2007. “Mechanical and Chemical Investigation of the Temperature Influence on the Tribological Mechanisms Occurring in OMC/Cast Iron Friction Contact”, Wear, v. 264, p. 815-825.

Day, A. J., Harding, P. R. J., Newcomb, T. P., 1984. “Combined Thermal and Mechanical Analysis of Drum Brakes”, Proceedings of the Institution of Mechanical Engineers, Part D: Journal of Automobile Engineering, v. 198, n 15, p. 287-294.

Day, A. J., 1988. “An Analysis of Speed, Temperature, and Performance Characteristics of Automotive Drum Brakes”, Journal of Tribology, v.110, p. 298-305.

Day, A. J., 1991. “Drum Brake Interface Pressure Distributions”, Proceedings of the Institution of Mechanical Engineers, Part D: Journal of Automobile Engineering, v. 205, n 2, p. 127-136.

Day, A. J., Tirovic, M., Newcomb, T. P., 1991. “Thermal Effects and Pressure Distributions in Brakes”, Proceedings of the Institution of Mechanical Engineers, Part D: Journal of Automobile Engineering, v. 205, n 3, p. 199-205.

Germany. “AK-Master Stand”. AK-Master, dezember of 1998. In Brake German Procedures.

Infantini, M. B., 2008. “Variáveis de Desempenho dos Sistemas de Freio”, Dissertação, Escola de Engenharia do Rio Grande do Sul.

Millner, N., Parsons, B., 1973. ”Effect of Contact Geometry and Elastic Deformations on the Torque Characteristics of a Drum Brake”, Proceedings of the Institution of Mechanical Engineers (London), v.187, n 26, 317-331.

Sanders, P. G., Dalka, T. M., Basch, R. H., 2001. “A Reduced-Scale Brake Dynamometer for Friction Characterization”, Tribology International, v. 34, p. 609-615.

Susin, V. A., Mazzaferro, J. A. E., Ferreira, N. F., Perondi, E. A., 2007. “Análise da Distribuição de Pressão de um Freio a Tambor com a Utilização do Método dos Elementos Finitos”, 8º Colloquium Internacional de Freios, 10 a 11 de maio, SAE Brasil.

Wilson, A. J, Belford, W. G, Bowsher G. T., 1968. “Testing Machines for Scale Vehicle Brake Installations”, The Engineer, p. 317-323.

Wilson, A. J., Bowsher, G. T., 1971. “Machine Testing for Brake Lining Classification”, Society of Automotive Engineers, paper 710249.

Yoshioka, O., 2007, “Análise dos Efeitos das Deformações Elásticas das Sapatas na Distribuição de Pressão de um Freio a Tambor”, Monografia, Escola de Engenharia - Universidade Federal do Rio Grande do Sul, Porto Alegre - RS, Brasil.

6. ACKNOWLEDGMENT

The authors wish to thank their colleagues Marcos Soares, Luciano Tedesco Matozo and Leandro at Fras-le S/A, who have provided assistance and suggestions.

7. RESPONSIBILITY NOTICE

The authors are the only responsible for the printed material included in this paper.